

Classification: BIOLOGICAL SCIENCES; Biophysics

Transient conformational fluctuation of TePixD during a reaction

Short title: Transient conformational fluctuation of TePixD

Kunisato Kuroi[†], Koji Okajima^{‡,§}, Masahiko Ikeuchi[‡], Satoru Tokutomi[§], and Masahide Terazima^{†,*}

[†]*Department of Chemistry, Graduate School of Science, Kyoto University, Kyoto 606-8502, Japan*

[‡]*Department of Life Sciences (Biology), Graduate School of Arts and Sciences, The University of Tokyo, Meguro, Tokyo 153-8902, Japan*

[§]*Research Institute for Advanced Science and Technology, Department of Biological Science, Graduate School of Science, Osaka Prefecture University, Sakai, Osaka 599-8531, Japan*

***Corresponding author**

Masahide Terazima

Department of Chemistry, Graduate School of Science, Kyoto University, Kyoto 606-8502, Japan

Tel/FAX: +81-75-753-4026

e-mail: mterazima@kuchem.kyoto-u.ac.jp

Abstract

Knowledge of the dynamical behavior of proteins, and in particular their conformational fluctuations, is essential to understanding the mechanisms underlying their reactions. Here, transient enhancement of the isothermal partial molar compressibility, which is directly related to the conformational fluctuation, during a chemical reaction of a blue-light sensor protein from the thermophilic cyanobacterium *Thermosynechococcus elongatus BP-1* (TePixD, T110078) was investigated in a time-resolved manner. The UV-Vis absorption spectrum of TePixD did not change with the application of high pressure. On the other hand, the TG signal intensities representing the volume change depended significantly on the pressure. This result implies that the compressibility changes during the reaction. From the pressure dependence of the amplitude, the compressibility change of two short-lived intermediate (I_1 and I_2) states were determined to be $+(5.6\pm 0.6)\times 10^{-2}\text{ cm}^3\text{ mol}^{-1}\text{MPa}^{-1}$ for I_1 and $+(6.6\pm 0.7)\times 10^{-2}\text{ cm}^3\text{ mol}^{-1}\text{MPa}^{-1}$ for I_2 . This result showed that the structural fluctuation of intermediates was enhanced during the reaction. To clarify the relationship between the fluctuation and the reaction, the compressibility of multiply excited TePixD was investigated. The isothermal compressibility of I_1 and I_2 intermediates of TePixD showed a monotonic decrease with increasing excitation laser power, and this tendency correlated with the reactivity of the protein. This result indicates that the TePixD decamer cannot react when its structural fluctuation is small. We concluded that the enhanced compressibility is an important factor for triggering the reaction of TePixD. This is the first report showing enhanced fluctuations of intermediate species during a protein reaction, supporting the importance of fluctuations.

Keywords:

fluctuation, photoreaction, protein

Significance statement

The role of conformational fluctuations in protein reactions has been frequently mentioned to discuss the reaction mechanism. Supporting evidences for the importance of the fluctuation have been reported by showing the relationship between the flexibility of the reactant structure and reaction efficiency. However, there has been no direct evidence showing that the fluctuation is indeed enhanced during the reaction, although recent molecular dynamic simulation pointed out the importance. Here, we focused our attention on the experimental proof of the enhancement by the time-resolved transient grating method, which is a unique and powerful method. Our result indeed showed that fluctuation is a key to understand why light stimulated proteins can transfer the signal without changing the averaged conformation.

¶body

Introduction

Proteins often transfer information through changes in domain–domain (or intermolecular) interactions. Photosensor proteins are an important example. They have light-sensing domains and function by utilizing the light-driven changes in domain–domain interactions (1). The sensor of blue light using FAD (BLUF) domain is a light-sensing module found widely among the bacterial kingdom (2). The BLUF domain initiates its photoreaction by the light-excitation of the flavin moiety inside the protein, which changes the domain–domain interaction, causing a quaternary structural change, and finally transmitting biological signals (3, 4). It has been an important research topic to elucidate how the initial photochemistry occurring in the vicinity of the chromophore leads to the subsequent large conformation change in other domains, which are generally apart from the chromophore.

It may be reasonable to consider that the conformation change in the BLUF domain is the driving force in its subsequent reaction; that is, the change in domain–domain interaction. However, sometimes, clear conformational changes have not been observed for the BLUF domain; its conformation is very similar before and after photoexcitation (5-13). The circular dichroism (CD) spectra of BLUF proteins AppA and TePixD did not change upon illumination (5, 13). Similarly, solution nuclear magnetic resonance (NMR) studies of AppA and BlrB showed only small chemical shifts upon excitation (9, 10). The solution NMR structure of BlrP1 showed a clear change, but this was limited in its C-terminal extension region, not core BLUF (11). Furthermore, the diffusion coefficient (D) of the BLUF domain of YcgF was not changed by photo-excitation (12) although D is sensitive to global conformational changes. These results imply that a minor structural change occurs in the BLUF domain. In such cases, how does the BLUF domain control its inter-domain interaction? Recently, an molecular dynamics (MD) simulation on another light-sensing domain, the light-oxygen-voltage (LOV) sensing domain suggested that fluctuation of the LOV core structure could be a key to understanding the mechanism of information transfer (14-16).

Because proteins work at room temperature, they are exposed to thermal fluctuations. The importance of such structural fluctuations for biomolecular reactions has been also pointed out, for example, enzymatic activity (17-20). Experimental detections of such conformation fluctuations using single molecular detection (21) or NMR techniques such as the hydrogen-deuterium (H-D) exchange, relaxation dispersion method and high-pressure NMR (22-24) have succeeded. However, these techniques could not detect the fluctuation of short-lived transient species. Indeed, single molecule spectroscopy can trace the fluctuation in real time, but it is still rather difficult to detect rapid fluctuations for a short-lived intermediate during a reaction. Therefore, information about the fluctuation of intermediates is so far limited.

A thermodynamic measurement is another way to characterize the fluctuation of proteins. In particular, the partial molar isothermal compressibility ($\bar{K}_T = -(\partial\bar{V}/\partial P)_T$) is essential, because this property is directly linked to the mean-square fluctuations of the protein partial molar volume by

$\langle(\bar{V} - \langle\bar{V}\rangle)^2\rangle \equiv \langle\delta\bar{V}^2\rangle = k_B T \bar{K}_T$ (25). (Here, $\langle X \rangle$ means the averaged value of a quantity of X.) Therefore, isothermal compressibility is thought to reflect the structural fluctuation of molecules (26). However, experimental measurement of this parameter of proteins in a dilute solution is quite difficult. Indeed, this quantity has been determined indirectly from the theoretical equation using the adiabatic compressibility of a protein solution, which was determined by the sound velocity in the solution (26-31). Although the relation between volume fluctuations and isothermal compressibility is rigorously correct only with respect to the intrinsic part of the volume compressibility, not the partial molar volume compressibility (32), we considered that this partial molar volume compressibility is still useful for characterizing the fluctuation of the protein structure including its interacting water molecules. In fact, the relationship between $\bar{\beta}_T$ and the volume fluctuation has been often used to discuss the fluctuation of proteins (17, 26-28) and the strong correlation of $\bar{\beta}_T$ of reactants with the functioning for some enzymes (17, 33, 34) has been reported. These studies show the functional importance of the structural fluctuation represented by $\bar{\beta}_T$. However, thermodynamic techniques lack time-resolution and it has been impossible to measure the fluctuations of short-lived intermediate species.

Recently, we have developed a time-resolving method for assessing thermodynamic properties using the pulsed laser induced transient grating (TG) method. Using this method, we have so far succeeded in measuring the enthalpy change (ΔH) (35-38), partial molar volume change ($\Delta\bar{V}$) (12, 35, 37), thermal expansion change ($\Delta\bar{\alpha}_{th}$) (12, 37), and heat capacity change (ΔC_p) (36-38) for short-lived species. Therefore, in principle, the partial molar isothermal compressibility change ($\Delta\bar{K}_T$) of a short-lived intermediate become observable if we conduct the TG experiment under the high-pressure condition and detect $\Delta\bar{V}$ with varying the external pressure.

There are several difficulties in applying the traditional high-pressure cell to the TG method to measure thermodynamic parameters quantitatively. The most serious problem is ensuring the quantitative performance of the intensity of TG signals measured under the high-pressure condition. On this point, our group has developed a new high-pressure cell specially designed for TG spectroscopy (39) and overcome this problem. In this paper, by applying this high-pressure TG system to the BLUF protein TePixD, we report the first measurement of $\Delta\bar{K}_T$ of short-lived intermediates to investigate the mechanism underlying signal transmission by BLUF proteins, from the view point of the transient fluctuation.

TePixD is a homolog of the BLUF protein PixD, which regulates the phototaxis of cyanobacterium (40), and exists in a thermophilic cyanobacterium *Thermocynechococcus elongates BP-1* (TII0078). TePixD is a relatively small (17-kDa) protein that consists only of the BLUF domain with two extended helices in the C-terminal region. In crystals and solutions, it forms a decamer that consists of two pentameric rings (41). The photochemistry of TePixD is typical among BLUF proteins (42-45); upon blue light illumination, the absorption spectrum shifts toward red by about 10 nm within a nanosecond. The absorption spectrum does not change further and the dark state is recovered with a time constant of ~ 5 s at room temperature (40, 43). The spectral red-shift was

explained by the rearrangement of the hydrogen bond network around the chromophore (6, 46-48). The TG method has revealed the dynamic photoreaction mechanism, which cannot be detected by conventional spectroscopic methods. The TG signal of TePixD (Fig.S-1) showed that there are two spectrally silent reaction phases: a partial molar volume expansion with the time constant of $\sim 40 \mu\text{s}$ and the diffusion coefficient (D) change with a time constant of $\sim 4 \text{ ms}$. Furthermore, it was reported that pentamer and decamer states of TePixD are in equilibrium, and that the final photoproduct of the decamer is pentamers generated by its dissociation (13, 49). On the basis of these studies, the reaction scheme has been identified as shown in Fig. 1. Here, I_1 is the intermediate of the spectrally red-shifted species (generated within a nanosecond) and I_2 is the one created upon the subsequent volume expansion process of $+4 \text{ cm}^3\text{mol}^{-1}$ ($\sim 40 \mu\text{s}$). Furthermore, an experiment of the excitation laser power dependence of its TG signal revealed that the TePixD decamer undergoes the original dissociation reaction when only one monomer in the decamer is excited (50). In this study, we investigated the transient compressibility of the intermediates I_1 and I_2 of the photoreaction of TePixD and found a direct link between their fluctuation and reactivity.

Results

Reaction detected by absorption at high pressures

Before measuring changes in compressibility, we first investigated the effects of pressure on the UV-Vis absorption spectra of TePixD in the dark state (Fig.S-2). Here, the spectrum was corrected to allow for the increase in density (i.e., concentration) of the solution owing to the increase in pressure (51). The absorption spectrum of TePixD was almost independent of the pressure. In addition, we checked the permanent pressure denaturation of TePixD by comparing the CD spectrum before and after applying the high pressure. The spectrum in a range of 200–250 nm recovered completely after the pressurization of 200 MPa. These results indicated that permanent pressure denaturation of TePixD did not occur in this pressure range.

The effect of pressure on the photochemistry of TePixD was investigated by the transient absorption (TA) method. The pressure dependence of the TA spectrum measured at $10 \mu\text{s}$ after excitation is shown in Fig. S-3. Here, the intensities were corrected using the absorbance change from the UV-Vis spectra at the excitation wavelength (462 nm). It is clear that the spectrum was not altered by pressure except for a slight decrease in amplitude. In addition, the time profiles of the TA signal of TePixD were probed at 483 nm under various pressures (Fig. S-4). The amplitude of the signal decreased slightly at high pressures, and the decay rate was increased. Because the TA spectrum was not altered by pressure, this slight decrease in amplitude was attributed to the quantum yield change. The quantum yield change (as the relative parameter ϕ/ϕ_0 (ϕ_0 : the quantum yield at 0.1 MPa)) and the lifetime (τ) of the dark recovery at various pressures were plotted (Fig.S-4(b) and (c)). The acceleration of the dark recovery and slight decrease in the quantum yield observed indicate the pressure effect to the transition state of the reaction. The pressure dependence of the rate is related with the activation volume along the reaction coordinate and this value is negative in this case. More

importantly for this study, we should point out that the pressure does not affect the reaction scheme of TePixD. Hence, we can discuss the fluctuation by measuring the volume change at various pressures.

Transient fluctuation during the reaction

We measured the TG signal for TePixD under the high-pressure condition to investigate the fluctuation of its intermediates at a weak light intensity, $1.02 \pm 0.02 \text{ mJ cm}^{-2}$, which is weak enough to excite only one monomer unit in the decamer (50). The time-evolution of the TG signal of TePixD after photoexcitation has been described previously (49). Here, we briefly summarize its essential feature. A typical TG signal at $q^2 = 3.5 \times 10^{12} \text{ m}^{-2}$ in a wide time range is depicted in Fig. S-1. The signal consists of the thermal grating component ($\sim 1 \text{ } \mu\text{s}$), a volume expansion process (weak decay after thermal diffusion ($\sim 40 \text{ } \mu\text{s}$)), and a peak of the molecular diffusion signal (2–20 ms), which represents the diffusion coefficient change. Analyzing the TG signal, we have determined the reaction scheme for TePixD (Fig. 1). In the present study, we applied high pressure and measured the TG signal representing the volume expansion process from an intermediate I_1 to I_2 (the amplified signal shown in the inset of Fig. S-1) to detect their fluctuations.

Fig. 2 shows the pressure dependence of the TG signal of the volume expansion process at $q^2 = 3.5 \times 10^{12} \text{ m}^{-2}$. It is clear that the TG signal of TePixD depended significantly on the pressure, in contrast to the results of UV-Vis and transient absorptions. As shown in SI-1, the TG signal in a longer time range of Fig.2 represents the protein diffusion signal, which has been analyzed by a sum of three exponential functions (49). However, in this study, we need only the amplitude of the volume grating signal, not the time profiles of the diffusion. Hence, in order to reduce the ambiguity of the fitting, we analyzed the diffusion signal by expanding the exponential function in the early time range and neglecting higher order terms of t (SI-4). The resultant fitting function is shown below.

$$I_{TG}(t) = \alpha(\delta n_{th} \exp(-D_{th}q^2t) + \delta n_V \exp(-k_Vt) + A + Bt)^2 \quad (1)$$

Here, α is a proportional constant, the first term of Eq. (1) represents the thermal diffusion process (δn_{th} ; thermal grating, D_{th} ; diffusion coefficient of the heat), the second term represents the volume expansion process (δn_V ; amplitude of the volume grating, k_V ; reaction rate of the volume change), and the last term ($A+Bt$) represents the contribution of the molecular diffusion signal. The TG signals at different pressures were fitted by Eq. (1) and fitting curves are shown by the solid lines in Fig.2. The fitting curves almost perfectly reproduced the signal and we could uniquely determine the parameters.

From the pressure dependence of the amplitude of species grating of I_1 and I_2 states, the pressure dependences of the volume changes ($\Delta \bar{V}_{g \rightarrow e}$) for I_1 and I_2 states were determined by a method described in SI-3 and shown in Fig.3, where $\Delta \bar{V}_{g \rightarrow e}$ for I_1 at 0.1 MPa was used as the reference value. We fitted the data by the following quadratic function.

$$\Delta \bar{V}_{g \rightarrow e}(P) = \Delta \bar{V}_{g \rightarrow e}(0.1) + \Delta \bar{K}_T P + (\partial \Delta \bar{K}_T / \partial P) P^2 \quad (2)$$

where P is the pressure, $\Delta\bar{V}_{g\rightarrow e}(0.1)$ is the volume difference at 0.1 MPa, $\Delta\bar{K}_T$ is the partial molar compressibility change compared to the ground state, and the last term is for the correction of the slight compressibility change by the pressure. From this fitting, we determined each parameter for I_1 and I_2 as follows: $\Delta\bar{K}_T = +(5.6\pm 0.6)\times 10^{-2}$ cm³mol⁻¹ MPa⁻¹ (for I_1) and $\Delta\bar{K}_T = +(6.6\pm 0.7)\times 10^{-2}$ cm³mol⁻¹ MPa⁻¹ (for I_2). Therefore, using the relationship between the compressibility and the volume fluctuation (i.e., $\Delta\langle(\bar{V} - \langle\bar{V}\rangle)^2\rangle = k_B T \Delta\bar{K}_T$), the volume fluctuation change from the ground state to the excited state ($\Delta\langle(\bar{V} - \langle\bar{V}\rangle)^2\rangle = \langle\delta\bar{V}^2\rangle$) was obtained to be 140 ± 20 (cm³ mol⁻¹)² for I_1 and 160 ± 20 (cm³ mol⁻¹)² for I_2 . (Here ‘mol’ means the number of excited monomers.) This result showed that the partial molar volume fluctuation of the short-lived intermediate states is larger than that of the ground state.

Compressibility of multi-excited species

To further examine the importance of the compressibility in the intermediate state of the reaction, we studied the laser power dependence of the compressibility changes. Previously, it was shown that photo-excitation of a monomer of TePixD yields I_1 and I_2 intermediates at any laser power, but does not produce the final product when multiple monomers in the decamer unit were excited. Therefore, if the structural fluctuation correlates with the reactivity of TePixD, examining the excitation power dependence of the compressibility will be a good test for it.

Fig. 4 shows the pressure dependence of the TG signal at $q^2 = 4.4\times 10^{12}$ m⁻² under four different excitation laser powers: 1.0, 7.9, 19, 27 mJ cm⁻². (For a negative control experiment, we measured the TG signal of a photo-inactive mutant (Q50A) under the same conditions (SI-6). Any volume change reaction was not observed for this mutant confirming that the above experimental conditions did not cause any artifact.) From the results shown in Fig. 4, it is clear that the TG signals became less sensitive to pressure with increasing excitation laser power. We fitted these TG signals at different powers by Eq. (1) and determined the compressibility of the intermediates in the similar way. The laser power dependence of the apparent compressibility change ($\Delta\bar{K}_T^{app}$) for I_1 and I_2 states obtained from the fitting is shown in Fig. 5 (a) and (b), respectively. For both states, the compressibility decreased monotonically with increasing the excitation laser power. Therefore, it is qualitatively apparent that a TePixD decamer (or pentamer) containing multiple excited monomers possesses smaller compressibilities than does a decamer containing only one excited monomer.

The observed compressibility change is the sum of contributions from a decamer having different numbers of excited monomers. To extract the compressibility change of multi-excited species, we fitted the results of Fig. 5 by the function of laser power as follows. The observed volume fluctuation is the sum of contributions from oligomers having different numbers of excited monomers. The apparent compressibility ($\Delta\bar{K}_T^{app}$) may be expressed as:

$$\Delta\bar{K}_T^{app} = \sum_{n\geq 1} n f_n \Delta\bar{K}_T^{(n)} \quad (3)$$

Here, f_n denotes the fraction of oligomers having n excited monomer units, and $\Delta\bar{K}_T^{(n)}$ is the

compressibility change of a monomer in that decamer. $\Delta\bar{K}_T^{(1)}$ was determined in the former section, but other parameters ($\Delta\bar{K}_T^{(n\geq 2)}$) are unknown. Hence, if we use this function to fit the laser power dependence in all power range, there are too many adjustable parameters to be determined uniquely. In order to avoid ambiguity for the fitting, we analyzed the data in a relatively weak laser power region as follows. In a laser power range of $< 8 \text{ mJcm}^{-2}$, the fraction of the triple excited species (f_3) is estimated to be smaller than 15 % of the total excited decamers (SI-5). The fraction of the species having $n > 3$ should be much smaller. Therefore, it may be reasonable to consider only $n=1$ and 2 for the fitting in a weak laser power region. In this case, Eq. (3) becomes

$$\Delta\bar{K}_T^{app} = f_1\Delta\bar{K}_T^{(1)} + f_2\Delta\bar{K}_T^{(2)} \quad (4)$$

Here, the fractions f_n are given by eq.(S-12) in SI-5, and the parameters c and I_s were fixed to the predetermined values described in (SI-5). For $\Delta\bar{K}_T^{(1)}$, we also fixed it to the values determined in the former section: $\Delta\bar{K}_T^{(1)} = 5.6 \times 10^{-2} \text{ cm}^3\text{mol}^{-1} \text{ MPa}^{-1}$ for I_1 and $6.6 \times 10^{-2} \text{ cm}^3\text{mol}^{-1} \text{ MPa}^{-1}$ for I_2 . Hence, Eq. (4) now contains only one adjustable parameter, $\Delta\bar{K}_T^{(2)}$. By using Eq. (4), we fitted the data in the laser power region below 8 mJcm^{-2} and the results are shown in Fig. 5. Although the adjustable parameter is only $\Delta\bar{K}_T^{(2)}$, the fitting curve well reproduced the laser power dependence in this region. From this fitting, the compressibility change of double-excited species ($\Delta\bar{K}_T^{(2)}$) was uniquely determined as $-(4.3 \pm 1.5) \times 10^{-2} \text{ cm}^3\text{mol}^{-1} \text{ MPa}^{-1}$ for I_1 and $-(6.7 \pm 2.4) \times 10^{-2} \text{ cm}^3\text{mol}^{-1} \text{ MPa}^{-1}$ for I_2 . The compressibility of both I_1 and I_2 of two-excited decamer was found to be much smaller than that of the one excited species, and even smaller than that of its ground state. Therefore, we concluded that the enhanced compressibility is important to lead to the dissociation reaction of TePixD decamer.

These results are schematically illustrated in Fig. 6.

Discussion

Traditionally, compressibility ΔK_T has been measured from the pressure dependence of the equilibrium constant at a pressure P , $K(P)$, which may be expressed by

$$\ln\left(\frac{K(P)}{K(0.1 \text{ MPa})}\right) = -\left(\frac{\Delta V}{RT}\right)P + \left(\frac{\Delta K_T}{2RT}\right)P^2 + \dots$$

Therefore, for a reaction under equilibrium between two states, the compressibility may be measured by the second-order expansion of P of the pressure dependent K . However, this traditional method cannot be applied to the short-lived intermediate species during chemical reactions in principle. Furthermore, higher pressure data is more important for determining the quadratic behavior of K . Therefore, this method may easily suffer from the effects of high pressure on protein structure (not the volumetric effect); that is, artifact. On the other hand, the present TG technique is more advanced; the volumetric data is directly determined from the signal intensity and the compressibility can be determined from the pressure effect in a low pressure range.

The detected enhancement of the compressibility was $5.6 \times 10^{-2} \text{ cm}^3\text{mol}^{-1} \text{ MPa}^{-1}$ for I_1 and $6.6 \times 10^{-2} \text{ cm}^3\text{mol}^{-1} \text{ MPa}^{-1}$ for I_2 . Although the compressibility in the ground stable state of TePixD has not yet been reported, we can roughly estimate how large the enhancement is compared with the

ground state as follows. According to the studies of Gekko *et al*, the square root of the volume fluctuation ($\sqrt{\langle(V - \langle V \rangle)^2\rangle}$) of globular proteins is about 0.3% of their partial molar volume (26), and the partial specific volumes of many globular proteins are very similar ranging from 0.7 to 0.75 cm³ g⁻¹. Using these data, the partial molar volume of the TePixD monomer is estimated to be ~13,000 cm³ mol⁻¹ assuming a partial specific volume of 0.75 cm³ g⁻¹. Therefore, its square root of the volume fluctuation in the ground state is calculated to be ~39 cm³ mol⁻¹. This value corresponds to the compressibility of 60×10⁻² cm³mol⁻¹MPa⁻¹ in the ground state. Therefore the observed enhancement of the compressibility (5.6×10⁻² and 6.6×10⁻² cm³mol⁻¹ MPa⁻¹ for I₁ and I₂ respectively) in the intermediate states is about 10% of the ground state compressibility for both I₁ and I₂.

We consider that the estimated increase of 10% in compressibility is large, because the fluctuation change may not be spread over the whole protein, but rather is localized in a small area, in particular, around the interface of TePixD pentamer rings, which must be important for the dissociation reaction. The light-induced structural change of the BLUF domain has been expected to occur in the C-terminal extension region of the BLUF domain; that is, from the β4-β5 loop to α4 helix (11, 52-54). However, in the case of TePixD, these regions are far from the interface of pentamer rings. Therefore, a structural change in these regions is insufficient to explain the dissociation of the decamer. Instead it may utilize the enhanced fluctuation of interface region to help achieve the dissociation reaction. In our previous study (50), we reported the discovery of the strange light intensity dependence. In this paper, we found that the 2 photon excitation suppress the fluctuation and concluded that this smaller fluctuation is a cause of the suppression of the reaction.

In conclusion, we succeeded in detecting isothermal partial molar compressibility of two short-lived intermediates during the photoreaction of TePixD. The enhancement of the volume fluctuation was observed for both I₁ and I₂ intermediate states and this enhancement should be the trigger for the dissociation reaction of the TePixD decamer. We believe this is the first direct experimental report to connect protein reactivity and fluctuations of reaction intermediates.

Methods

Sample preparation

TePixD was expressed using a pET28a vector transformed into *Escherichia coli* BL21 (DE3) and purified by nickel affinity column chromatography, as reported previously (40). In all measurements, the sample was prepared by dissolving in HEPES buffer (20 mM HEPES-NaOH (pH 7.5), 500 mM NaCl). The concentration of TePixD was determined by UV-Vis absorption measurement, using the extinction coefficient of FAD; $\epsilon = 11,300 \text{ M}^{-1} \text{ cm}^{-1}$ at 450 nm. In most cases, the sample concentration used was ~530 μM.

High-pressure equipment

Details of the high-pressure apparatus used in this study have been described elsewhere (39). The pressure resistance of this cell is up to 500 MPa. In all measurements, the internal temperature was

set to be 295.5 K and the applied pressure range was from 0.1 MPa to 200 MPa. It has been validated that this high pressure cell can achieve the complete reproducibility of a TG signal with applying high pressure and the sample replacement operation (39).

Transient absorption (TA) measurement

The TA signals were monitored after photo-excitation by a XeCl excimer laser-pumped dye laser beam (Lambda Physik CompexPro102; $\lambda = 308$ nm, Lumonics Hyper Dye 300; $\lambda = 462$ nm). A Xe lamp was used to measure the TA spectra. The probe light passing through the sample was focused on an optical fiber, leading to a monochromator (ACTON Research Corporation SpectraPro 2300i). The temporal profile of the TA signal was monitored by a probe light from a light-emitting diode (LED Luminar; Nissin Electronic Co., Tokyo, Japan) at a wavelength of 483 nm with the FWHM of 16 nm, which was selected by long-pass glass filters. This light was detected by a photomultiplier tube (R1477; Hamamatsu). The signal was fed into a digital oscilloscope (TDS-7104; Tektronix) and averaged 20 times. The repetition rate for excitation was set to 0.025 Hz.

TG measurement under high pressure

Detailed descriptions on the TG method are described in the section SI-3 of the supporting information. Briefly, in the TG method, two laser pulses are introduced into the sample solution to trigger the photoreaction. The intensity (I_{TG}) is proportional to the square of the generated refractive index change (δn) arising from the volume change, temperature change and absorption change. The experimental set up for TG measurement was similar to that reported before (12, 35-39, 49, 50). The excitation laser pulse and detection systems (a photomultiplier tube and digital oscilloscope) were all same as those used for measuring the time-profile of the TA signal. CW diode laser (835 nm; Crysta Laser) was used as a probe beam. The grating wave-number q in the experimental condition was determined from the thermal grating signal of a calorimetric reference sample (bromocresol purple in water) measured under the same condition. The repetition rate for excitation was set to 0.04 Hz, which is slower than the dark recovery time of TePixD (~ 5 s). Whenever we applied high pressure, we always reset the pressure to 0.1 MPa after every compression to check the recovery of the signal. It was confirmed that the TG signals were completely reversible. The excitation laser power was monitored using a pyroelectric Joulemeter (Coherent, J3-09).

References

1. Zoltowski BD & Gardner KH (2010) Tripping the Light Fantastic: Blue-Light Photoreceptors as Examples of Environmentally Modulated Protein–Protein Interactions. *Biochemistry* 50(1):4-16.
2. Losi A & Gartner W (2008) Bacterial bilin- and flavin-binding photoreceptors. *Photochemical & photobiological sciences : Official journal of the European Photochemistry Association and the European Society for Photobiology* 7(10):1168-1178.
3. Masuda S (2013) Light Detection and Signal Transduction in the BLUF Photoreceptors. *Plant and Cell Physiology* 54(2):171-179.
4. Losi A & Gartner W (2012) The evolution of flavin-binding photoreceptors: an ancient chromophore serving trendy blue-light sensors. *Annual review of plant biology* 63:49-72.
5. Kraft BJ, *et al.* (2003) Spectroscopic and Mutational Analysis of the Blue-Light Photoreceptor AppA: A Novel Photocycle Involving Flavin Stacking with an Aromatic Amino Acid†. *Biochemistry* 42(22):6726-6734.
6. Masuda S, Hasegawa K, Ishii A, & Ono TA (2004) Light-induced structural changes in a putative blue-light receptor with a novel FAD binding fold sensor of blue-light using FAD (BLUF); Slr1694 of *synechocystis* sp. PCC6803. *Biochemistry* 43(18):5304-5313.
7. Anderson S, *et al.* (2005) Structure of a novel photoreceptor, the BLUF domain of AppA from *Rhodobacter sphaeroides*. *Biochemistry* 44(22):7998-8005.
8. Majerus T, Kottke T, Laan W, Hellingwerf K, & Heberle J (2007) Time-Resolved FT-IR Spectroscopy Traces Signal Relay within the Blue-Light Receptor AppA. *ChemPhysChem* 8(12):1787-1789.
9. Grinstead JS, *et al.* (2006) The solution structure of the AppA BLUF domain: insight into the mechanism of light-induced signaling. *Chembiochem : a European journal of chemical biology* 7(1):187-193.
10. Wu Q, Ko WH, & Gardner KH (2008) Structural requirements for key residues and auxiliary portions of a BLUF domain. *Biochemistry* 47(39):10271-10280.
11. Wu Q & Gardner KH (2009) Structure and insight into blue light-induced changes in the BlrP1 BLUF domain. *Biochemistry* 48(12):2620-2629.
12. Nakasone Y, Ono TA, Ishii A, Masuda S, & Terazima M (2010) Temperature-sensitive reaction of a photosensor protein YcgF: possibility of a role of temperature sensor. *Biochemistry* 49(10):2288-2296.
13. Kuroi K, *et al.* (2013) Anomalous diffusion of TePixD and identification of the photoreaction product. *Photochemical & Photobiological Sciences*.
14. Freddolino PL, Dittrich M, & Schulten K (2006) Dynamic switching mechanisms in LOV1 and LOV2 domains of plant phototropins. *Biophysical journal* 91(10):3630-3639.
15. Freddolino PL, Gardner KH, & Schulten K (2013) Signaling mechanisms of LOV domains: new insights from molecular dynamics studies. *Photochemical & Photobiological Sciences*.
16. Peter E, Dick B, & Baeurle S (2012) Signals of LOV1: a computer simulation study on the

- wildtype LOV1-domain of *Chlamydomonas reinhardtii* and its mutants. *Journal of molecular modeling* 18(4):1375-1388.
17. Gekko K, Obu N, Li J, & Lee JC (2004) A Linear Correlation between the Energetics of Allosteric Communication and Protein Flexibility in the *Escherichia coli* Cyclic AMP Receptor Protein Revealed by Mutation-Induced Changes in Compressibility and Amide Hydrogen–Deuterium Exchange†. *Biochemistry* 43(13):3844-3852.
 18. Eisenmesser EZ, *et al.* (2005) Intrinsic dynamics of an enzyme underlies catalysis. *Nature* 438(7064):117-121.
 19. Bhabha G, *et al.* (2011) A Dynamic Knockout Reveals That Conformational Fluctuations Influence the Chemical Step of Enzyme Catalysis. *Science (New York, N.Y.)* 332(6026):234-238.
 20. Kitahara R, *et al.* (2012) A Delicate Interplay of Structure, Dynamics, and Thermodynamics for Function: A High Pressure NMR Study of Outer Surface Protein A. *Biophysical journal* 102(4):916-926.
 21. Deniz AA, Mukhopadhyay S, & Lemke EA (2008) Single-molecule biophysics: at the interface of biology, physics and chemistry. *Journal of The Royal Society Interface* 5(18):15-45.
 22. Hwang T-L, van Zijl PM, & Mori S (1998) Accurate Quantitation of Water-amide Proton Exchange Rates Using the Phase-Modulated CLEAN Chemical EXchange (CLEANEX-PM) Approach with a Fast-HSQC (FHSQC) Detection Scheme. *J Biomol NMR* 11(2):221-226.
 23. Mittermaier A & Kay LE (2006) New Tools Provide New Insights in NMR Studies of Protein Dynamics. *Science (New York, N.Y.)* 312(5771):224-228.
 24. Akasaka K, Kitahara R, & Kamatari YO (2013) Exploring the folding energy landscape with pressure. *Archives of Biochemistry and Biophysics* 531(1–2):110-115.
 25. Cooper A (1976) Thermodynamic fluctuations in protein molecules. *Proceedings of the National Academy of Sciences of the United States of America* 73(8):2740-2741.
 26. Gekko K (2002) Compressibility gives new insight into protein dynamics and enzyme function. *Biochimica et Biophysica Acta (BBA) - Protein Structure and Molecular Enzymology* 1595(1–2):382-386.
 27. Gekko K & Noguchi H (1979) Compressibility of globular proteins in water at 25.degree.C. *The Journal of Physical Chemistry* 83(21):2706-2714.
 28. Gekko K & Hasegawa Y (1986) Compressibility-structure relationship of globular proteins. *Biochemistry* 25(21):6563-6571.
 29. Sarvazyan AP (1991) Ultrasonic Velocimetry of Biological Compounds. *Annual Review of Biophysics and Biophysical Chemistry* 20(1):321-342.
 30. Kharakoz DP (1997) Partial Volumes and Compressibilities of Extended Polypeptide Chains in Aqueous Solution: Additivity Scheme and Implication of Protein Unfolding at Normal and High Pressure. *Biochemistry* 36(33):10276-10285.
 31. Taulier N & Chalikian TV (2002) Compressibility of protein transitions. *Biochimica et Biophysica Acta (BBA) - Protein Structure and Molecular Enzymology* 1595(1–2):48-70.

32. Son I, Selvaratnam R, Dubins DN, Melacini G, & Chalikian TV (2013) Ultrasonic and Densimetric Characterization of the Association of Cyclic AMP with the cAMP-Binding Domain of the Exchange Protein EPAC1. *The Journal of Physical Chemistry B* 117(37):10779-10784.
33. Kamiyama T & Gekko K (2000) Effect of ligand binding on the flexibility of dihydrofolate reductase as revealed by compressibility. *Biochimica et Biophysica Acta (BBA) - Protein Structure and Molecular Enzymology* 1478(2):257-266.
34. Gekko K & Yamagami K (1998) Compressibility and Volume Changes of Lysozyme due to Inhibitor Binding. *Chemistry Letters* 27(8):839-840.
35. Inoue K, Sasaki J, Morisaki M, Tokunaga F, & Terazima M (2004) Time-resolved detection of sensory rhodopsin II-transducer interaction. *Biophysical journal* 87(4):2587-2597.
36. Khan JS, Imamoto Y, Kataoka M, Tokunaga F, & Terazima M (2005) Time-Resolved Thermodynamics: Heat Capacity Change of Transient Species during Photoreaction of PYP. *Journal of the American Chemical Society* 128(3):1002-1008.
37. Eitoku T, *et al.* (2007) Photochemical intermediates of Arabidopsis phototropin 2 LOV domains associated with conformational changes. *Journal of molecular biology* 371(5):1290-1303.
38. Hazra P, Inoue K, Laan W, Hellingwerf KJ, & Terazima M (2008) Energetics and role of the hydrophobic interaction during photoreaction of the BLUF domain of AppA. *The journal of physical chemistry. B* 112(5):1494-1501.
39. Hoshihara Y, Kimura Y, Matsumoto M, Nagasawa M, & Terazima M (2008) An optical high-pressure cell for transient grating measurements of biological substance with a high reproducibility. *The Review of scientific instruments* 79(3):034101.
40. Okajima K, *et al.* (2005) Biochemical and functional characterization of BLUF-type flavin-binding proteins of two species of cyanobacteria. *Journal of biochemistry* 137(6):741-750.
41. Kita A, Okajima K, Morimoto Y, Ikeuchi M, & Miki K (2005) Structure of a cyanobacterial BLUF protein, Tll0078, containing a novel FAD-binding blue light sensor domain. *Journal of molecular biology* 349(1):1-9.
42. Laan W, van der Horst MA, van Stokkum IH, & Hellingwerf KJ (2003) Initial characterization of the primary photochemistry of AppA, a blue-light-using flavin adenine dinucleotide-domain containing transcriptional antirepressor protein from *Rhodobacter sphaeroides*: a key role for reversible intramolecular proton transfer from the flavin adenine dinucleotide chromophore to a conserved tyrosine? *Photochemistry and photobiology* 78(3):290-297.
43. Fukushima Y, Okajima K, Shibata Y, Ikeuchi M, & Itoh S (2005) Primary intermediate in the photocycle of a blue-light sensory BLUF FAD-protein, Tll0078, of *Thermosynechococcus elongatus* BP-1. *Biochemistry* 44(13):5149-5158.
44. Gauden M, *et al.* (2005) Photocycle of the flavin-binding photoreceptor AppA, a bacterial transcriptional antirepressor of photosynthesis genes. *Biochemistry* 44(10):3653-3662.
45. Okajima K, *et al.* (2006) Fate determination of the flavin photoreceptions in the cyanobacterial blue light receptor TePixD (Tll0078). *Journal of molecular biology* 363(1):10-18.

46. Bonetti C, *et al.* (2009) The role of key amino acids in the photoactivation pathway of the *Synechocystis* Slr1694 BLUF domain. *Biochemistry* 48(48):11458-11469.
47. Domratcheva T, Grigorenko BL, Schlichting I, & Nemukhin AV (2008) Molecular models predict light-induced glutamine tautomerization in BLUF photoreceptors. *Biophysical journal* 94(10):3872-3879.
48. Gauden M, *et al.* (2006) Hydrogen-bond switching through a radical pair mechanism in a flavin-binding photoreceptor. *Proceedings of the National Academy of Sciences of the United States of America* 103(29):10895-10900.
49. Tanaka K, *et al.* (2009) Oligomeric-state-dependent conformational change of the BLUF protein TePixD (Tll0078). *Journal of molecular biology* 386(5):1290-1300.
50. Tanaka K, *et al.* (2011) A way to sense light intensity: Multiple-excitation of the BLUF photoreceptor TePixD suppresses conformational change. *FEBS letters* 585(5):786-790.
51. Saul A & Wagner W (1989) A Fundamental Equation for Water Covering the Range from the Melting Line to 1273 K at Pressures up to 25 000 MPa. *Journal of Physical and Chemical Reference Data* 18(4):1537-1564.
52. Hasegawa K, Masuda S, & Ono TA (2005) Spectroscopic analysis of the dark relaxation process of a photocycle in a sensor of blue light using FAD (BLUF) protein Slr1694 of the cyanobacterium *Synechocystis* sp. PCC6803. *Plant & cell physiology* 46(1):136-146.
53. Khrenova M, Domratcheva T, Grigorenko B, & Nemukhin A (2011) Coupling between the BLUF and EAL domains in the blue light-regulated phosphodiesterase BlrP1. *Journal of molecular modeling* 17(7):1579-1586.
54. Barends TR, *et al.* (2009) Structure and mechanism of a bacterial light-regulated cyclic nucleotide phosphodiesterase. *Nature* 459(7249):1015-1018.

Figure captions

Fig. 1 Schematic illustration of the photoreaction of TePixD. Yellow circles represent the TePixD monomer in the ground state, which constructs the decamer and pentamer states. In the dark state, these two forms are in equilibrium. The excited, spectral red-shifted state of the TePixD monomer is indicated by a red circle. The square represents the I₂ state of the monomer, which is created by the volume expansion process.

Fig. 2 Typical TG signals of TePixD in the sub-millisecond time region, which represents the volume expansion process from the intermediate I₁ to I₂, recorded at every 25 MPa from 0.1 MPa to 200 MPa (from bottom to upper) with $q^2 = 3.5 \times 10^{12} \text{ m}^{-2}$. Fitting curves based on the fitting function Eq. (1) are shown by black solid lines. Pressures are indicated by the legend in the figure.

Fig. 3 Pressure dependence of the volume change from the ground state (g) to the excited state (e) (i.e., $\Delta \bar{V}_{g \rightarrow e}$) for I₁ and I₂ states. Because the absolute value of $\Delta \bar{V}_{g \rightarrow e}$ of I₁ and I₂ are not known, their pressure dependences in this figure are plotted by relative values from $\Delta \bar{V}_{g \rightarrow e}$ of I₁ at 0.1 MPa. Solid lines represent the best fitting results by a quadratic function of Eq. (2).

Fig. 4 Similar TG signals for TePixD to those in **Fig. 3** under four different laser power conditions of 1.0, 7.9, 19, 27 mJ /cm². Applied pressures were 0.1 (red), 50 (orange), 100 (green), 150 (blue), and 200 MPa (magenta). The grating wave number was $q^2 = 4.4 \times 10^{12} \text{ m}^{-2}$. Signal intensities with different excitation laser powers were normalized by the obtained fitting parameter δn_v of Eq. (1) at 0.1 MPa, which is proportional to the number of excited species. Fitting curves based on the fitting function Eq. (1) are shown by solid lines.

Fig.5 Laser power dependence of the volume fluctuation change from the ground state to the excited state I₁ (a) and I₂ (b). Best-fit curves by Eq. (4) are shown by the solid lines.

Fig. 6 Schematic illustration of the volume fluctuation change from the ground state, depicted along the reaction coordinate of TePixD for both cases in which one monomer is excited (red lines) or multiple monomers are excited (blue lines). In the figure, volume fluctuation change is expressed per mol of TePixD monomers.

Fig. 1

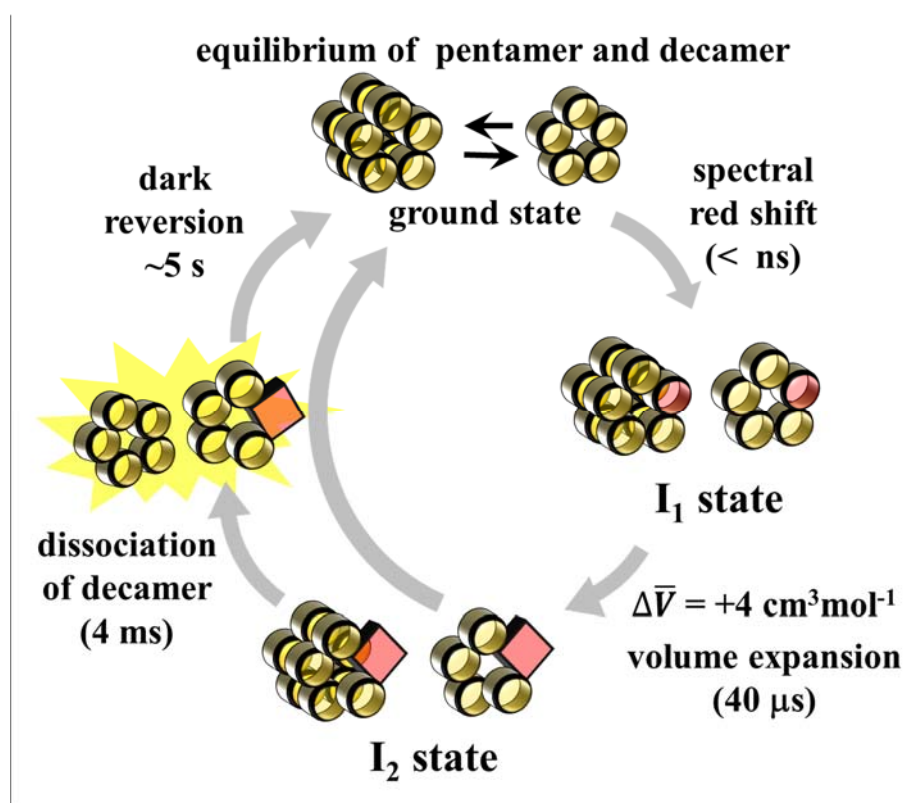


Fig. 2

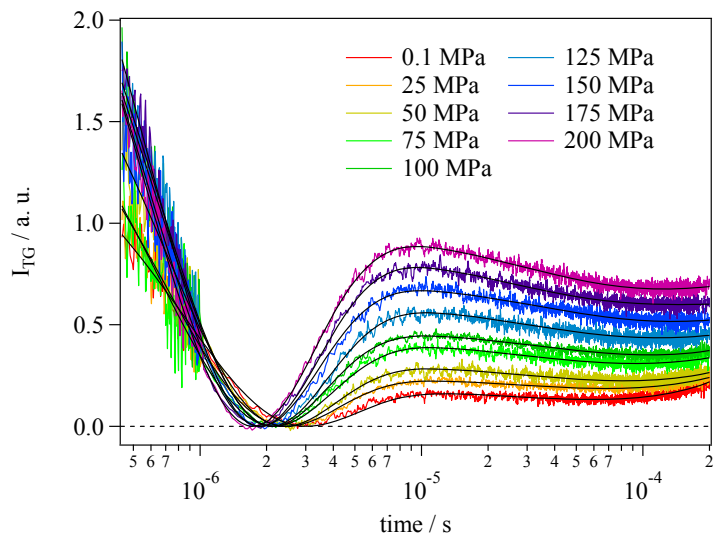


Fig.3

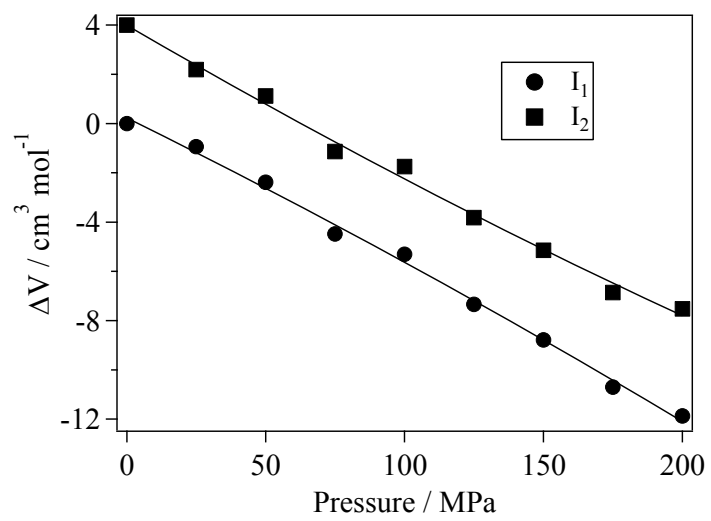


Fig. 4

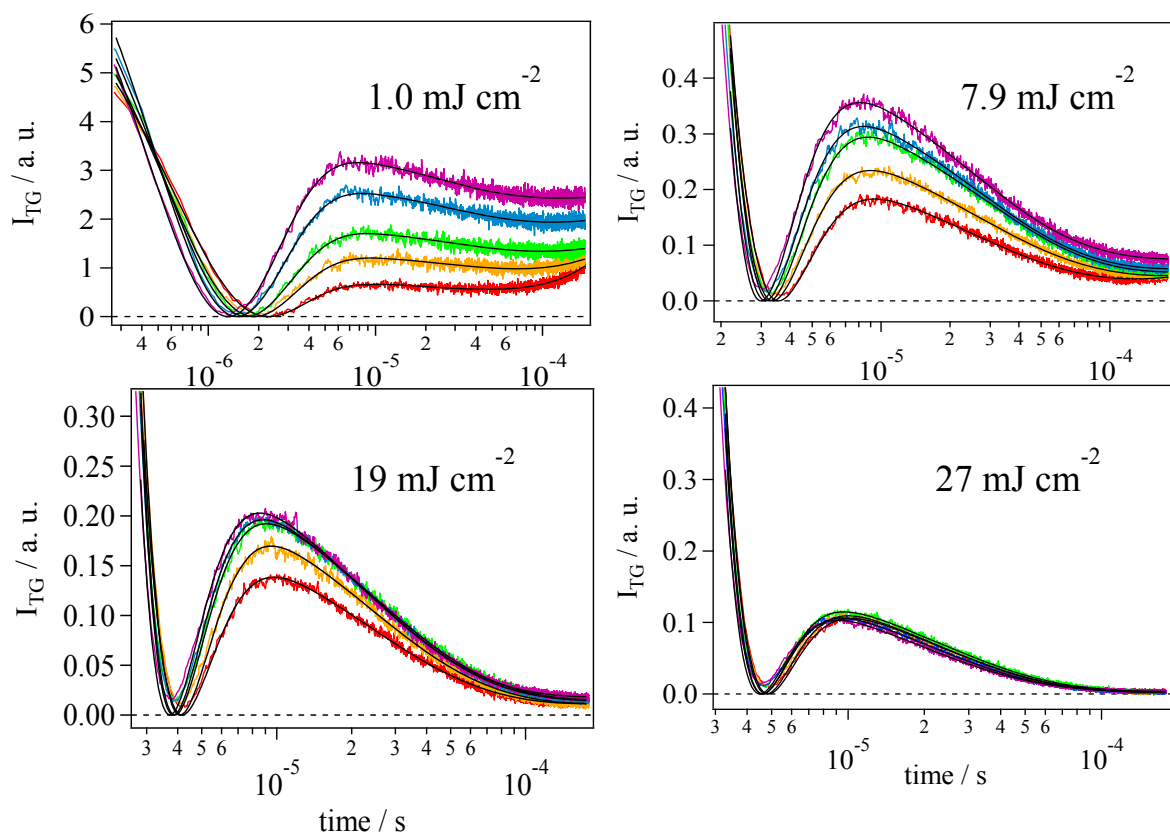


Fig. 5

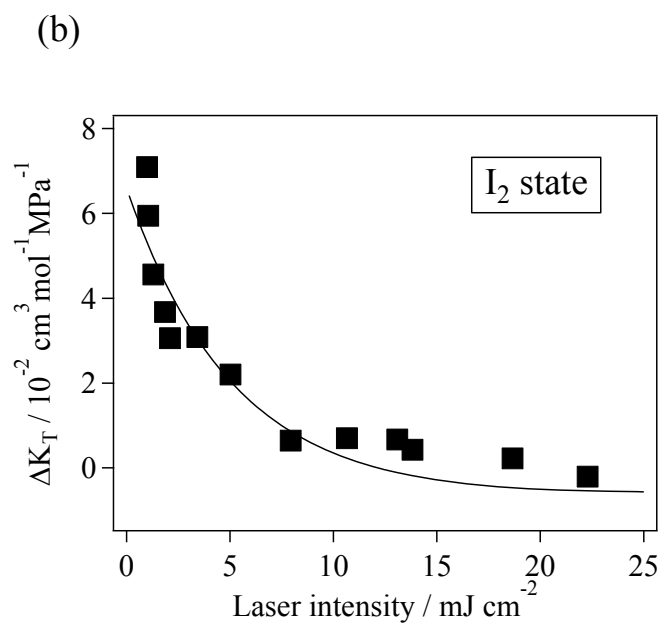
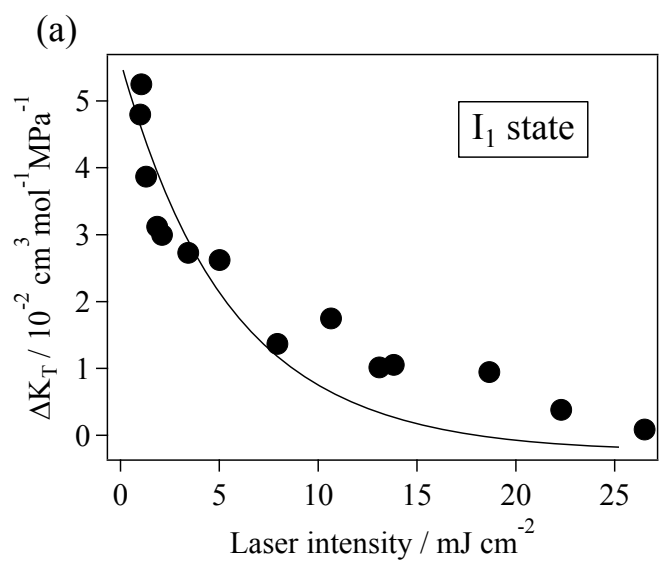
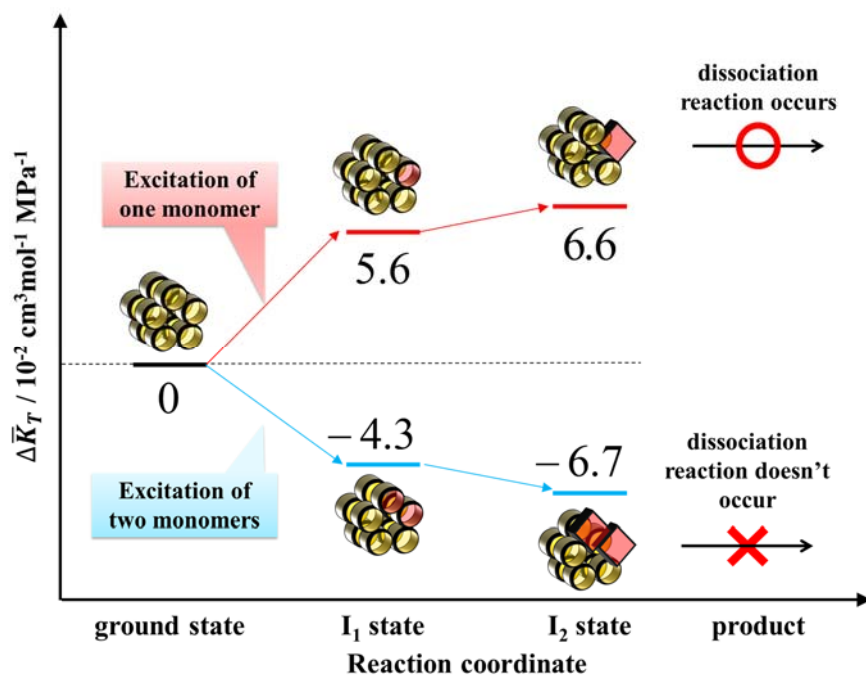


Fig. 6



Transient conformational fluctuation of TePixD during a reaction

Kunisato Kuroi[†], Koji Okajima^{‡,§}, Masahiko Ikeuchi[‡], Satoru Tokutomi[§], and Masahide Terazima^{†,*}

[†]*Department of Chemistry, Graduate School of Science, Kyoto University, Kyoto 606-8502, Japan*

[‡]*Department of Life Sciences (Biology), Graduate School of Arts and Sciences, The University of Tokyo, Meguro, Tokyo 153-8902, Japan*

[§]*Research Institute for Advanced Science and Technology, Department of Biological Science, Graduate School of Science, Osaka Prefecture University, Sakai, Osaka 599-8531, Japan*

SI-1. TG signal of TePixD at 0.1 MPa

Typical TG signal of TePixD in the wide time region from sub-microseconds to seconds measured at 0.1 MPa. Detailed analysis and features of this TG signal has been described elsewhere (1).

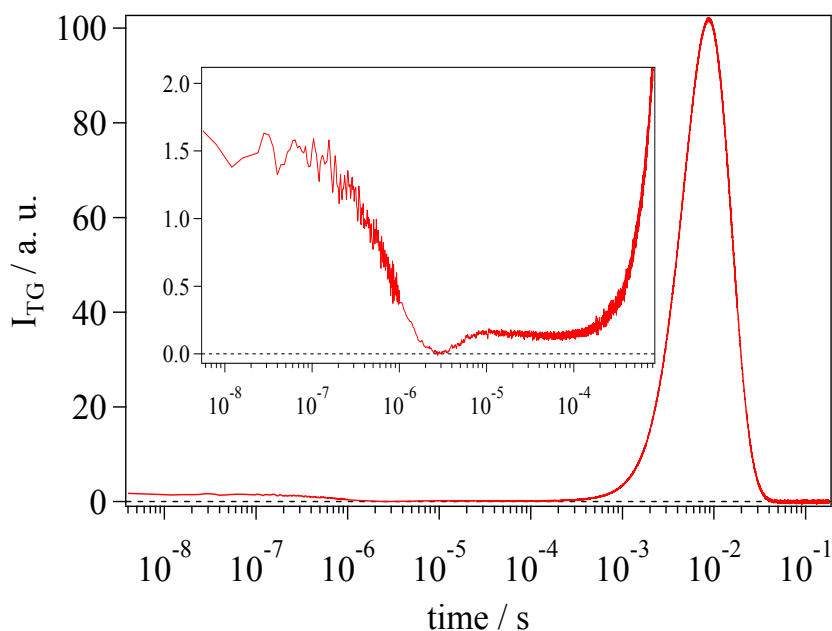


Fig. S-1 Typical TG signal of TePixD in the wide time region from sub-microseconds to seconds measured at 0.1 MPa with the grating wavenumber of $q^2 = 3.5 \times 10^{12} \text{ m}^{-2}$. The inset shows the amplified TG signal in a fast time region. The signal consists of the thermal grating component ($\sim 1 \mu\text{s}$), the volume expansion process (weak decay after the thermal diffusion ($\sim 40 \mu\text{s}$)), and a peak of the molecular diffusion signal (2 ms - 20 ms), which represents the change in diffusion coefficient.

SI-2. Absorption spectrum of TePixD

UV-Vis absorption spectra of TePixD, transient absorption difference spectra after the photoexcitation at various pressures are depicted below.

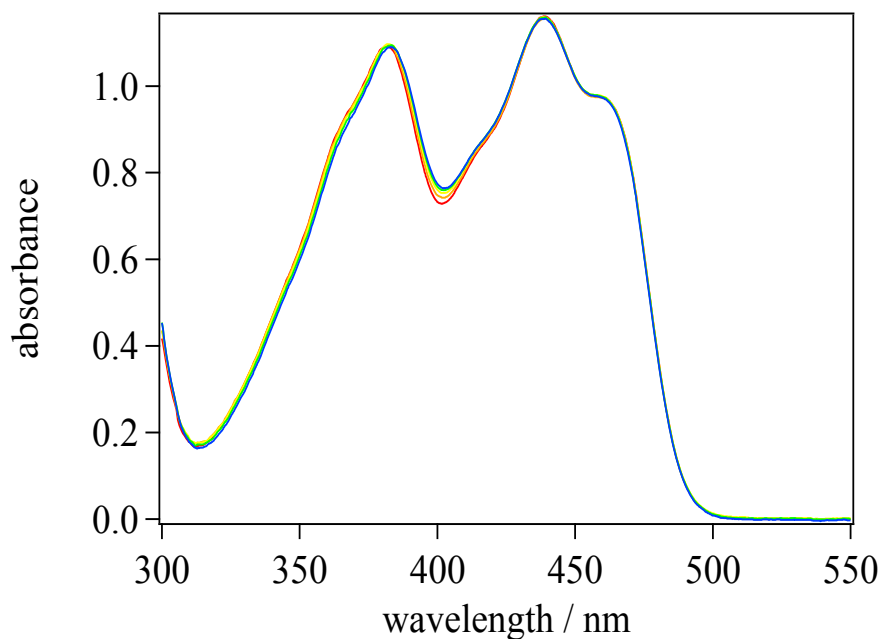


Fig. S- 2 UV-Vis absorption spectra of TePixD in the buffer solution at 0.1 MPa (red), 50 MPa (orange), 100 MPa (yellow), 150 MPa (green), 200 MPa (blue). The intensity was corrected for the density change.

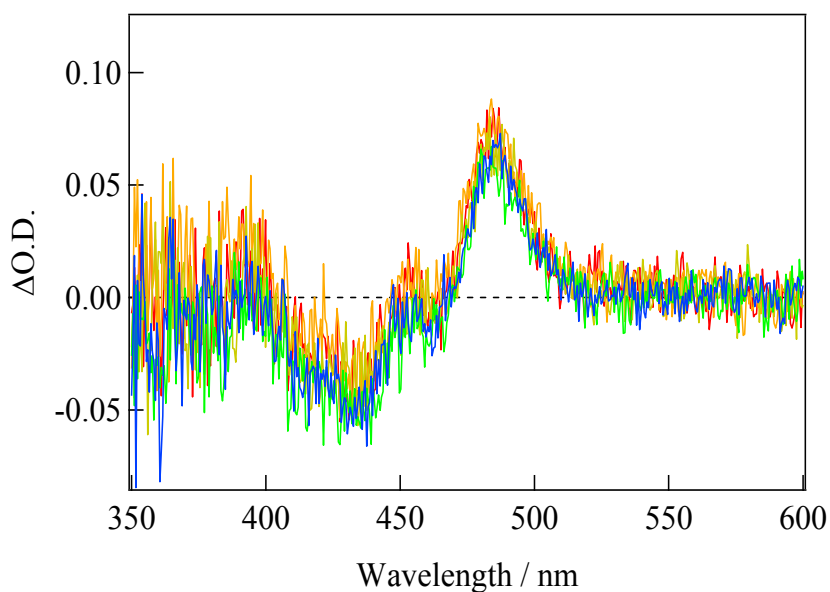


Fig. S-3 Transient absorption difference spectra (light minus dark) of TePixD recorded at 10 μ s after excitation by the nanosecond-pulsed laser of 462 nm, at 0.1 MPa (red), 50 MPa (orange), 100 MPa (yellow), 150 MPa (green), 200 MPa (blue). These intensities were corrected for the absorbance change at the excitation wavelength (462 nm).

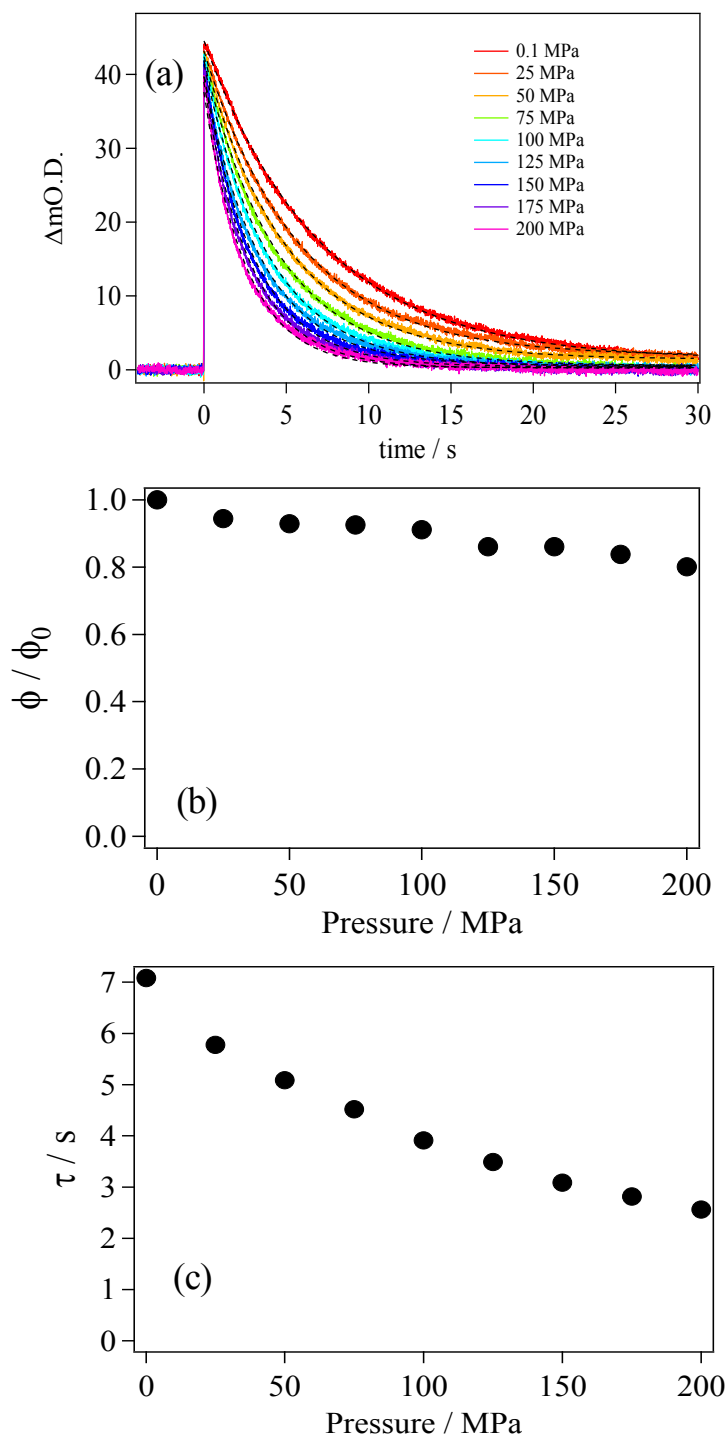


Fig. S-4 (a) Temporal profiles of the transient absorption of TePixD after excitation at 462 nm recorded at

every 25 MPa from 0.1 MPa to 200 MPa. Pressures are shown in the legend in the figure. The best-fit curves by a single-exponential function are shown by broken lines. (b) Pressure dependence of the relative quantum yield (ϕ_0 is the quantum yield at 0.1 MPa) of the photoreaction of TePixD, obtained from each amplitude of the time profiles of (a). (c) Pressure dependence of the time constant for the dark recovery of TePixD

SI-3. Principles

Detailed principles of the TG method have been reported previously (2, 3). Here, we briefly introduce only the basic concepts and principles that are necessary to understand this study. In the TG method, the refractive index change (δn), which is generated by the photo-excitation of chemical species, is detected as the intensity of a diffracted probe beam. This diffracted beam is the TG signal. Under a weak diffraction condition and a condition where the probe beam is not absorbed, the intensity of the TG signal ($I_{TG}(t)$) is proportional to the square of δn . The refractive index change arises from two factors owing to the temperature increase of the solution by the heat release (thermal grating; δn_{th}) and photo-chemical reactions of the excited species (species grating; δn_{spe}), both of which are generally time-dependent. Therefore,

$$I_{TG}(t) = \alpha[\delta n_{th}(t) + \delta n_{spe}(t)]^2 \quad (S - 1)$$

where α is an experimental constant reflecting the sensitivity of the set up. α has been validated to be constant even under the application of pressure (4).

The amplitude of the thermal grating is proportional to the thermal energy released from the photo-excited molecules, and δn_{th} is expressed as

$$\delta n_{th} = \frac{dn}{dT} \frac{h\nu\phi W}{\rho C_p} \Delta N \quad (S - 2)$$

where ΔN is the number of reaction molecules in a unit volume (mol L^{-1}), ϕ is the quantum yield of the thermal releasing process, $h\nu$ is the photon energy of the excitation light (J mol^{-1}) and followings are parameters of the solvent water; W is the molecular weight (g mol^{-1}), n is the refractive index, ρ is the density (g L^{-1}), C_p is the heat capacity ($\text{J K}^{-1} \text{mol}^{-1}$). For a calorimetric reference sample that releases photon energy promptly as thermal energy without any reaction, ϕ is unity.

The species grating δn_{spe} consists of two contributions: the changes in the partial molar volume (δn_V : the volume grating) and the changes in the absorption spectrum (δn_{pop} : population grating). The volume grating (δn_V) is given by

$$\delta n_V = \left(V \frac{dn}{dV} \Phi \Delta N \right) \Delta \bar{V} \quad (\text{S} - 3)$$

where Φ is the quantum yield of the reaction, $\Delta \bar{V}$ is the partial molar volume change induced by the photoreaction ($\text{cm}^3 \text{mol}^{-1}$), and V is the molar volume of the solution. Here we approximate it by the molar volume of water. $\Delta \bar{V}$ was calculated by taking a ratio of δn_V to δn_{th} of the calorimetric reference (δn_{th}^{ref}) (i.e., dividing Eq. (S-3) by Eq. (S-2)) measured under the same condition as the sample. Then $\Delta \bar{V}$ is expressed as

$$\Delta \bar{V} = \left(\frac{1}{V} \frac{dV}{dT} \right) \frac{h \nu W}{\rho C_p \Phi} \left(\frac{\delta n_V}{\delta n_{th}^{ref}} \right) = \frac{\alpha_{solv} h \nu W}{\rho C_p \Phi} \left(\frac{\delta n_V}{\delta n_{th}^{ref}} \right) \quad (\text{S} - 4)$$

where α_{solv} represents the thermal expansion coefficient of the solvent, and Φ is the quantum yield of the photoreaction of TePixD, which has been reported to be 0.29 (5). The physical parameters of the solvent water (α_{solv} , W , ρ , C_p) were obtained from the literature. With only the experimental values in the last parentheses, $\Delta \bar{V}$ was determined.

Transient compressibility of reaction intermediates can be obtained from the pressure dependence of the species grating (δn_{spe}). Of the two components of the species grating (δn_{pop} and δn_V), δn_{pop} can be regarded as pressure-independent, because the transient absorption of TePixD was almost independent of pressure. Therefore, providing that ‘ Δ ’ represents any change caused by pressure, we obtain

$$\Delta \delta n_{spe} = \Delta(\delta n_{pop} + \delta n_V) \approx \Delta \delta n_V \quad (\text{S} - 5)$$

Here δn_V is related to the partial molar volume change given in Eq. (S-3). Regarding the term in the parentheses in Eq. (S-3), we confirmed that $\Phi \Delta N$ was almost constant under high pressures by the transient absorption method. dn/dV can be also regarded as constant because the pressure dependences of both the refractive index (n) and the partial molar volume (V) of the water are negligibly small. Hence, the proportional constant between $\Delta \bar{V}$ and $\Delta \delta n_V$ in Eq. (S-3) can be regarded as constant. Then, we obtain from Eq. (S-5)

$$\Delta \delta n_{spe} \approx \Delta \delta n_V \approx \left(V \frac{dn}{dV} \Phi \Delta N \right) \Delta \Delta \bar{V}_{g \rightarrow e} \quad (\text{S} - 6)$$

where $\Delta \bar{V}_{g \rightarrow e}$ means the volume change from the ground state to the excited state. If we know the volume change in Eq. (S-3) at 0.1 MPa, we can determine $\Delta \Delta \bar{V}_{g \rightarrow e}$ at any pressure by comparing $\Delta \delta n_{spe}$ with δn_V of 0.1 MPa. With the pressure dependence of $\Delta \bar{V}_{g \rightarrow e}$, the compressibility change between the ground and excited states ($\Delta \bar{K}_{g \rightarrow e}$) was finally determined by Eq. (S-7):

$$-\frac{d\Delta\bar{V}_{g\rightarrow e}}{dP} = \Delta\bar{K}_{g\rightarrow e} \quad (\text{S} - 7)$$

Using the fitting parameters of Eq. (1), the species grating (δn_{spe}) for I_1 and I_2 states of TePixD can be expressed as $\delta n(I_1) = \delta n_V + A$ and $\delta n(I_2) = A$, where A is defined by eq.(S-9) in SI-4. Here, we determined the volume change ($\Delta\bar{V}$) corresponding to δn_V as $\Delta\bar{V} = 4\pm 0.5 \text{ cm}^3$ per 1 mol of TePixD monomer by taking the ratio of δn_V to the thermal grating (δn_{th}) of the calorimetric reference. Therefore, an increase (or decrease) in δn_{spe} provides the pressure-induced change in δn_V (i.e., $\Delta\delta n_V$), and it further provides the changes in $\Delta\bar{V}_{g\rightarrow e}$ with changing pressure.

SI-4. derivation of Eq. (1).

The molecular diffusion signal of TePixD is generally expressed by the below two-state model equation, which assumes the reaction scheme that the reactant (R) is converted to the intermediate (I) immediately by photo-excitation and the product (P) is produced from I at the reaction rate of k (i.e.; $R \xrightarrow{h\nu} I \xrightarrow{k} P$). The mathematical expression of the two-state model is as follows (2):

$$I_{TG}(t) = \alpha[\delta n_I \exp\{-(D_I q^2 + k)t\} + \delta n_P \frac{k}{(D_P - D_I)q^2 - k} [\exp\{-(D_I q^2 + k)t\} - \exp(-D_P q^2 t)] - \delta n_R \exp(-D_R q^2 t)]^2 \quad (\text{S} - 8)$$

The diffusion coefficient (D) of each species and reaction rate k have been reported as $D_R = 4.9 \times 10^{-11} \text{ m}^2 \text{ s}^{-1}$, $D_I = 4.4 \times 10^{-11} \text{ m}^2 \text{ s}^{-1}$, $D_P = 3.2 \times 10^{-11} \text{ m}^2 \text{ s}^{-1}$, and $k = 250 \text{ s}^{-1}$. In the observation time here ($t < 2 \times 10^{-4} \text{ s}$) and the grating wave number ($q^2 = 3.5 \times 10^{12} \text{ m}^{-2}$), each term in the exponential function ($(D_I q^2 + k)t$, $D_P q^2 t$, $D_R q^2 t$) becomes smaller than 0.1. Then, each exponential term can be well approximated as $e^{\alpha x} \approx 1 + \alpha x$, and we obtain a much simpler expression:

$$I_{TG}(t) = \alpha(A + Bt)^2$$

$$(A = \delta n_I - \delta n_R \quad B = (\delta n_P - \delta n_I)k + (\delta n_R D_R - \delta n_I D_I)q^2) \quad (\text{S} - 9)$$

This is a simplified expression to fit the diffusion signal in a fast time range. Taking the other two components (thermal diffusion signal and volume change signal) into account, we obtain (S-10) (Eq. (1) in main text):

$$I_{TG}(t) = \alpha(\delta n_{th} \exp(-D_{th} q^2 t) + \delta n_V \exp(-k_V t) + A + Bt)^2 \quad (\text{S} - 10)$$

where the first term represents the thermal diffusion process (δn_{th} : thermal grating, D_{th} : diffusion coefficient of the heat), the middle term represents the volume expansion process (δn_V : volume grating, k_V : rate constant of the volume change from I_1 to I_2), the last term ($A + Bt$) represents the contribution of

the molecular diffusion signal, and α is a proportional constant.

SI-5. Derivation of the expression of f_n .

f_n can be written using the equation of Poisson distribution (P_n) as follows. When λ monomers in the oligomer are excited on average, the probability that n monomers in an oligomer are excited is described as

$$P_n = \frac{\exp(-\lambda) \cdot \lambda^n}{n!} \quad \text{where } \lambda = \frac{cI}{1 + I/I_s} \quad (\text{S} - 11)$$

(I : laser intensity (mJ/cm^2), c : constant I_s : saturation intensity).

Previously, it was reported that δn_R determined from the molecular diffusion signal of TePixD is proportional to P_1 (6). In this study, δn_R at 0.1 MPa was determined at various laser powers (I) (Fig. S-5). It should be noted that δn_R corresponds to the relative number of decamers that produced the final product. This laser power dependence was well fitted by aP_1 (a : proportional constant) and we determined the parameters as $a = 2.88 \pm 0.08$, $I_s = 37.2 \pm 10 \text{ mJ cm}^{-2}$, and $c = 0.215 \pm 0.016$.

The probability that an oligomer absorbs at least one photon is expressed as $1 - P_0$. Hence, f_n should be expressed as

$$f_n = \frac{P_n}{1 - P_0} = \frac{\exp(-\lambda)}{1 - \exp(-\lambda)} \frac{\lambda^n}{n!} \quad (\text{S} - 12)$$

Using the determined parameters in λ (i.e., c and I_s), the calculated f_n (from $n = 1$ to $n = 5$) at each excitation laser power is shown in Fig S-6. From this calculation, we estimated that the fraction of triple excited species (f_3) is smaller than 15 % of the total excited decamers below 8 mJcm^{-2} .

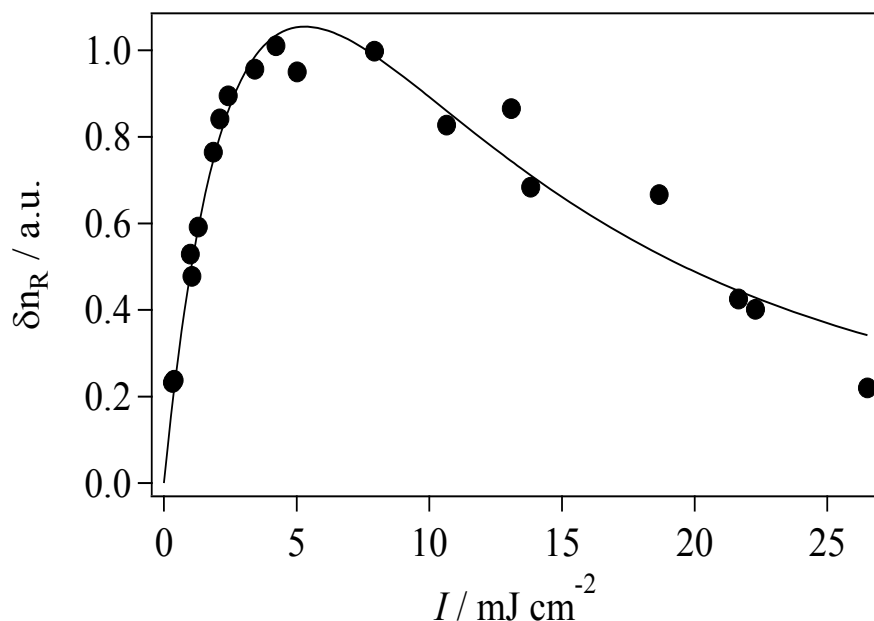


Fig. S-5 Laser power dependence of δn_R determined from the intensity of the molecular diffusion peak of the TG signal. δn_R corresponds to the relative number of decamer molecules that underwent the diffusion coefficient change. The solid curve is the best fit line using the equation of Poisson distribution ($n = 1$ in Eq. S-11).

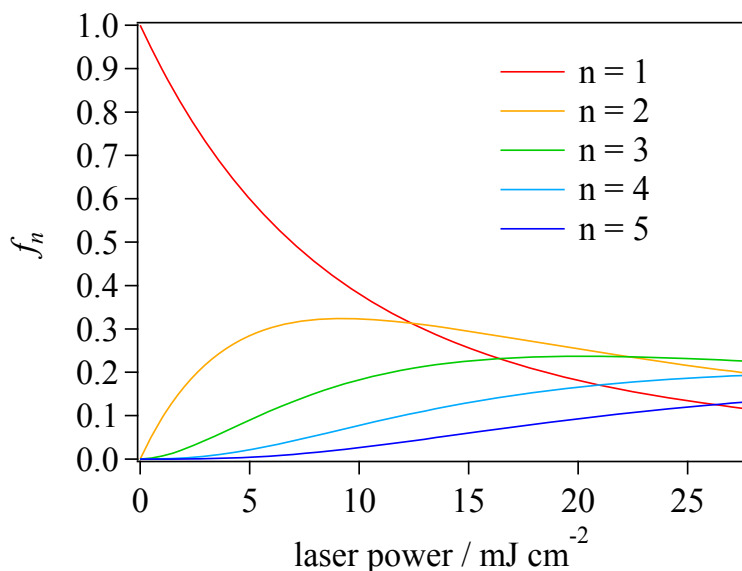


Fig. S-6 Laser power dependence of the fraction of n -excited species (from $n = 1$ to $n = 5$) calculated by Eq. (S-12). The number n are shown by the legend in the figure.

SI-6. TG signal of photo-inactive mutant of TePixD (Q50A).

For a negative control experiment, we measured the TG signal of a photo-inactive mutant of TePixD (Q50A). The key glutamine residue for the BLUF photoreaction was replaced by alanine in this mutant, and it has been shown that this mutant does not create the spectral red shift species (i.e., this is a photo-inactive mutant) (7). For this mutant, we have expected that there is no volume change and the dissociation reaction, so that we should not observe any TG signal except the thermal grating. We prepared Q50A TePixD mutant in the way described elsewhere (7, 8). Site-directed mutagenesis to generate Q50A TePixD mutant was performed using PCR-based QuickChange site-directed mutagenesis kit (Stratagene) with primers (sense, 5'-GGCATGTTTCTGgcAACCCCTTGAGGGC-3' and antisense, 5'-GCCCTCAAGGGTTgcCAGAAACATGCC-3'). The plasmid carrying the desired substitution was confirmed using nucleotide sequencing with BigDye terminator fluorescence detection method (Applied Biosystems) and a capillary sequencer (PRISM 310 Genetic Analyzer; Applied Biosystems). The expression and purification was performed in the same way as that of WT TePixD.

As expected, the TG signal after photoexcitation of this mutant consisted of only the thermal grating signal. Figure S-7 shows the comparison of the TG signal of the wild type (WT) representing the volume change, and the Q50A mutant in the same time range under the same condition (at 500 μM , $q^2 = 4.68 \times 10^{12} \text{ m}^{-2}$, laser intensity of 13 mJ/cm^2). This result confirms that the experimental conditions in our experiment (even at the high laser intensity and high concentration) did not cause any artifact in the signal.

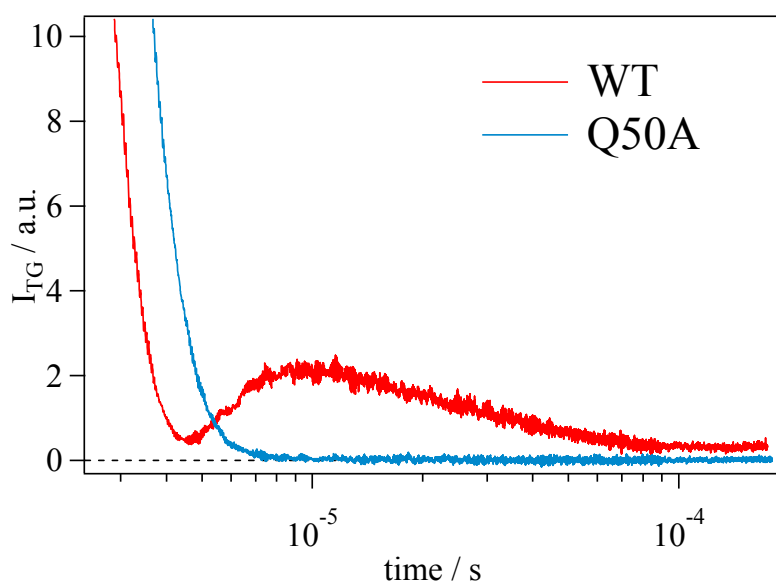


Fig. S-7 The TG signals of the wild type (red line: WT) and the Q50A mutant (blue line) of TePixD measured under the same condition at 13 mJ/cm^2 . (The signals decaying in microseconds time range for both samples are the thermal grating component.)

References

1. Tanaka K, *et al.* (2009) Oligomeric-state-dependent conformational change of the BLUF protein TePixD (Tll0078). *Journal of molecular biology* 386(5):1290-1300.
2. Terazima M (2006) Diffusion coefficients as a monitor of reaction kinetics of biological molecules. *Physical chemistry chemical physics : PCCP* 8(5):545-557.
3. Terazima M (2002) Molecular volume and enthalpy changes associated with irreversible photo-reactions. *Journal of Photochemistry and Photobiology C: Photochemistry Reviews* 3(2):81-108.
4. Hoshihara Y, Kimura Y, Matsumoto M, Nagasawa M, & Terazima M (2008) An optical high-pressure cell for transient grating measurements of biological substance with a high reproducibility. *The Review of scientific instruments* 79(3):034101.
5. Fukushima Y, Okajima K, Shibata Y, Ikeuchi M, & Itoh S (2005) Primary intermediate in the photocycle of a blue-light sensory BLUF FAD-protein, Tll0078, of *Thermosynechococcus elongatus* BP-1. *Biochemistry* 44(13):5149-5158.

6. Tanaka K, *et al.* (2011) A way to sense light intensity: Multiple-excitation of the BLUF photoreceptor TePixD suppresses conformational change. *FEBS letters* 585(5):786-790.
7. Okajima K, *et al.* (2006) Fate determination of the flavin photoreceptions in the cyanobacterial blue light receptor TePixD (Tll0078). *Journal of molecular biology* 363(1):10-18.
8. Kita A, Okajima K, Morimoto Y, Ikeuchi M, & Miki K (2005) Structure of a cyanobacterial BLUF protein, Tll0078, containing a novel FAD-binding blue light sensor domain. *Journal of molecular biology* 349(1):1-9.